Journal of Marine Science and Application (2022) 21: 134-144
https://doi.org/10.1007/s11804-022-00302-w

RESEARCH ARTICLE

Numerical Analysis of Local Joint Flexibility of K-joints with External Plates Under Axial Loads in Offshore Tubular Structures

Hossein Nassiraei[1] and Amin Yara[1]

Received: 29-Jul-2022 / Accepted: 19-Sep-2022

Abstract

The Local Joint Flexibility (LJF) of steel K-joints reinforced with external plates under axial loads is investigated in this paper. For this aim, firstly, a finite element (FE) model was produced and verified with the results of several experimental tests. In the next step, a set of 150 FE models was generated to assess the effect of the brace angle (θ), the stiffener plate size (η and λ), and the joint geometry (γ, τ, ξ, and β) on the LJF factor (f_{LJF}). The results showed that using the external plates can decrease 81% of the f_{LJF}. Moreover, the reinforcing effect of the reinforcing plate on the f_{LJF} is more remarkable in the joints with smaller β. Also, the effect of the γ on the f_{LJF} ratio can be ignored. Despite the important effect of the f_{LJF} on the behavior of tubular joints, there is not available any study or equation on the f_{LJF} in any reinforced K-joints under axial load. Consequently, using the present FE results, a design parametric equation is proposed. The equation can reasonably predict the f_{LJF} in the reinforced K-joints under axial load.

Keywords Local joint flexibility; K-joints; Axial load; External stiffener plates; Parametric study; Design formula

1 Introduction

Tubular members, because of their high capacity and convenient equipment installation, are extensively used in the support system of offshore structures such as jackets and jack-ups (Lu et al., 2020). These tubular structural members are connected by the welding process which leads to tubular joints. As an intrinsic feature of a tubular joint, the local joint flexibility (LJF) is one of the factors affecting the dynamic response and global static of an offshore structures. The LJF decreases the buckling loads, increases the deflections, changes the natural frequencies, and redistributes the nominal stresses of the structure (Ahmadi and Mayeli, 2018; Underwater Engineering Group, 1985; Bouwkamp et al., 1980). Consequently, the conventional methods for the analysis and design of the tubular joints may not be reliable enough. Because, they assume that the joints are rigid. This local deformation would decrease the capacity of the joint by redistributing the member-end moments and loads compared with the usual rigid joint. This results in reducing the cost (Gao et al., 2013; Nassiraei, 2017). Hence, it is important to investigate the LJF of tubular joints with a reliable method.

Khan et al. (2016 and 2018), Asgarian et al. (2014), Fessler et al. (1986), Buitrago et al. (1993), Nassiraei and Yara (2022) indicated that ratio of the chord dimeter to brace diameter (β), the ratio of chord radius to chord thickness (γ), the ratio of brace thickness to chord thickness (τ), and the brace angle (θ) have the most influential parameters in joint flexibility of K-joints. Also, Nassiraei and Rezadoost (2021a) showed that the reinforcing plate thickness and length have effect on the joint flexibility of joints reinforced with the reinforcing plates.

In this paper, firstly, a numerical model was created and validated with the results of 16 experimental tests. In the numerical models, the weld connecting the brace to the chord was generated. In the next step, a set of 150 K-joints (Figure 1) was numerically simulated to investigate the effect of the reinforcing plate size (η and λ), the joint geome-

Article Highlights

- 150 FE models were produced to evaluate the LJF in CHS K-joints with plates under axial load;
- The effect of the θ, β, γ, ξ, and τ, λ, and η is evaluated;
- A design formula is proposed to determine the f_{LJF}.

✉ Hossein Nassiraei
h.nassiraei@guilan.ac.ir

[1] Department of Civil Engineering, Faculty of Engineering, University of Guilan, Guilan, Iran

try (β, ξ, γ, and τ), and the brace angle (θ) on the f_{LJF} of the reinforced joints ($f_{\mathrm{LJF,\,s}}$) and the ratio of the $f_{\mathrm{LJF,\,s}}$ to the f_{LJF} of the corresponding un-reinforced joint ($f_{\mathrm{LJF,\,u}}$). The parameters (η, λ, γ, θ, β, τ, and ξ) are applied to relate the f_{LJF} of the reinforced K-joint. The parameters are shown in Figure 1. After investigating the effect of each parameter on the f_{LJF}, a detailed f_{LJF} database was prepared and finally, a parametric equation was derived. It can be safely utilized for constructing and reinforcing the joints in offshore structures.

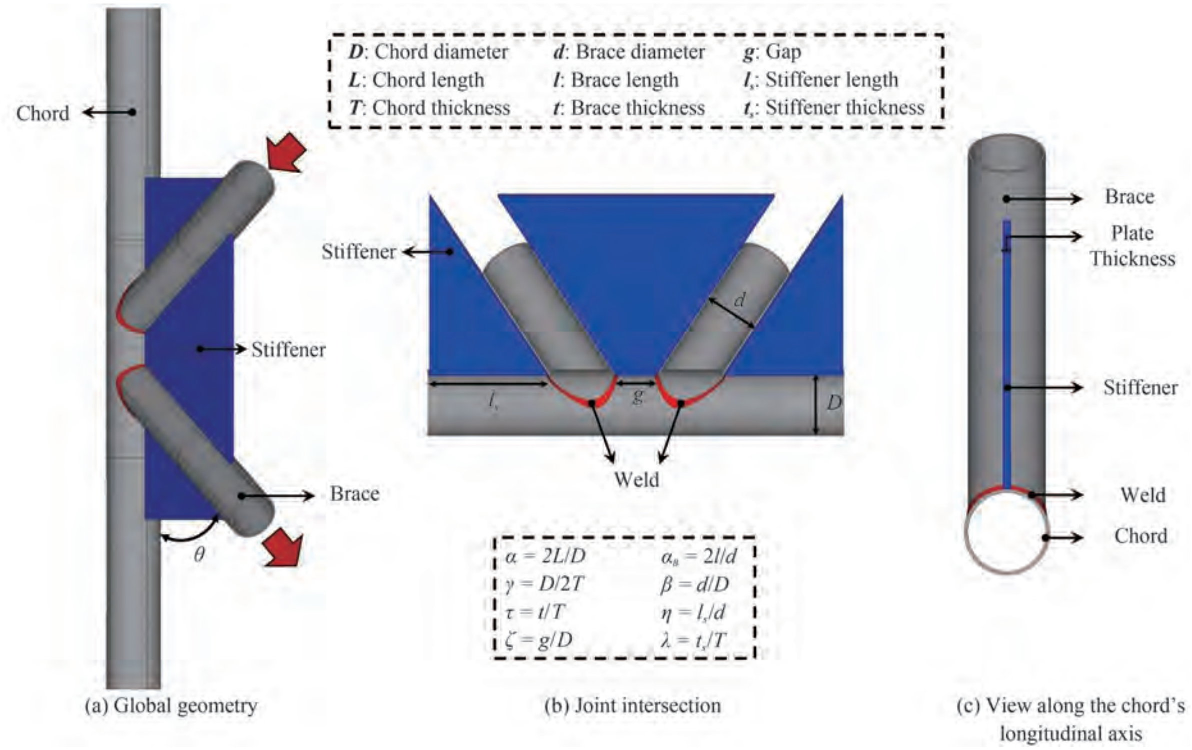

Figure 1 K-joint reinforced with the outer plate

2 Literature review

No study is carried out on the LJF in K-joints with any methods under axial load. However, some works are conducted on the LJF in un-reinforced K-joints. Fessler et al. (1986a) assessed the f_{LJF} in un-reinforced multi-brace tubular joints. Asgarian et al. (2014) and Buitrago et al. (1993) studied the LJF of K-joints. In these works, just one brace was subjected to force. In addition, Khan et al. (2016) compared past studies on the f_{LJF} in un-reinforced K-joints. Chen et al. (1990) established some equations to determine the f_{LJF} in CHS K-joints.

Nassiraei and Yara (2022) investigated the effect of the external plate on the f_{LJF} in K-joints under bending loads. Nassiraei and Rezadoost (2021b) investigated the effect of the external plate and fiber reinforced polymer on the f_{LJF} in joints. Also, they established some equations for calculating the f_{LJF}. Furthermore, some other works are carried out on the static capacity of tubular T- and X-joints reinforced with the external plates. Li et al. (2018), Ding et al. (2018), and Zhu et al. (2017) showed that the reinforcing plate can increase the ultimate strength of X- and T-joints. Also, other methods can be used for reinforced tubular joints, such as collar plates (Nassiraei et al. 2018; Nassiraei et al. 2019; Nassiraei 2019a), doubler plates (Nassiraei et al. 2016; Nassiraei et al. 2017), fiber reinforced polymers (Nassiraei and Rezadoost 2021c; Nassiraei and Rezadoost 2021d; Nassiraei and Rezadoost 2021e; Nassiraei and Rezadoost 2021f), and external ring (Nassiraei and Rezadoost 2022a; Nassiraei and Rezadoost 2022b).

Fessler et al. (1986b) conducted several experimental T- and Y-models under axial, OPB, and IPB loads. They established some equations for determining the f_{LJF}. Also, the LJF in T/Y-joints was studied by Efthymiou (1985). Martins and Silva (2015) investigated the effect of LJF on the offshore structure behavior. Also, the works of Mishra et al. (2021), Kumar et al. (2015), Chaubey et al. (2018a), and Chaubey et al. (2018b) can be mentioned.

It can be concluded from the preceding paragraphs that the effect of none of the reinforcing techniques on the f_{LJF} in K-joints under axial load has been investigated. Consequently, there is an essential requirement for investigating so that concrete guidelines on LJF evaluation in retrofitted K-joints with the external plates can be formulated. Figure 1 presents a K-joint reinforced with the external plates. This retrofitting technique can be applied to structures during design and operation.

3 Definition of the f_{LJF}

For the joins under axial load, the LJF can be defined as:

$$\mathrm{LJF} = (\Delta / P)\sin\theta \tag{1}$$

where P is the brace load, Δ is the average local deformation normal to the chord axis. It can be determined by Eq. (2). Also, the θ is the brace angle (Figure 1).

$$\Delta = \frac{(\Delta_1 - \Delta'_1) + (\Delta_2 - \Delta'_2) + (\Delta_3 - \Delta'_3) + (\Delta_4 - \Delta'_4)}{4} \tag{2}$$

The positions of $\Delta_1 - \Delta_4$ and $\Delta'_1 - \Delta'_4$ are showed in Figure 2. For relating the LJF to the joint's geometry, a coefficient named the f_{LJF} is defined. For the tubular K-joints in axial load, the f_{LJF} can be obtained using Eq. (3).

$$f_{LJF} = (\Delta / P)ED\sin\theta \tag{3}$$

where, E is Young's modulus.

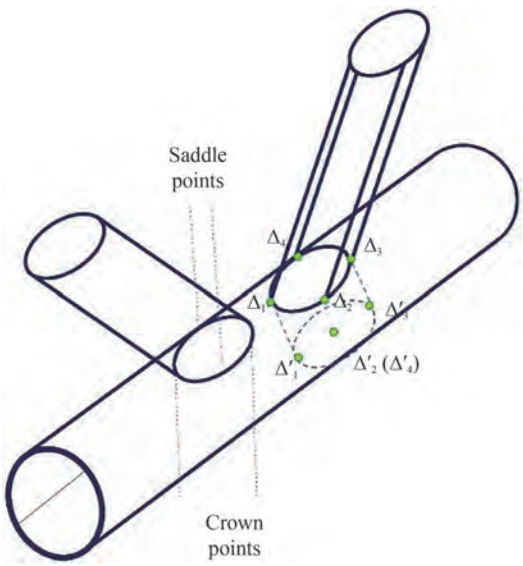

Figure 2 Points of measured deformation on the joint

4 FE modeling and validation

ANSYS Ver. 20 was used for the numerical simulation. The recommendations of AWS (2005) were utilized to design the welds, as previous works (Nassiraei and Rezadoost 2020; Nassiraei and Rezadoost 2021g; Nassiraei and Rezadoost 2021h). The generated weld can be seen in Figures 1 and 3 (red color). To mesh of the chord, welds, braces, and plates, the SOLID185 element was applied. Figure 3 depicts a meshed K-joint with the external plates. In Figures 3 and 4, the stiffener plates are shown in blue color. The balanced loads were applied to the brace ends (Figure 1a). Also, the displacements of the chord ends were fixed. Moreover, the linear static analysis was used to obtain the f_{LJF} (Nassiraei 2020; Nassiraei 2022). Also, Lostado Lorza et al. (2015), Lostado Lorza et al. (2018), 2017, and Íñiguez Macedo et al. (2019) were used to solve some of the key questions and points for meshing and boundary conditions.

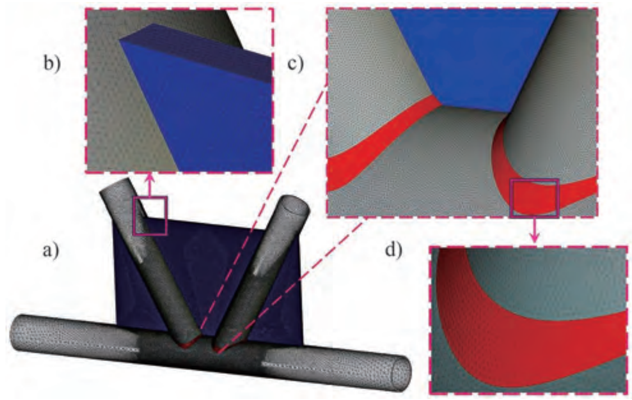

Figure 3 Generated mesh in the reinforced K-joint: (a) Reinforced joint, (b) and (c) Joint intersection and (d) weld profile

Until now, no experimental data of f_{LJF} for K-joints with any reinforcing method is available. Therefore, bellow experimental data are utilized to confirm the present FE model:

- The f_{LJF} of 11 T/Y-joints under axial load
- The load-displacement curve of two X-joints reinforced with the external plates under tension
- The force-displacement curve of two X-joints with the external plates under compression
- The load-displacement curve of one T-joints with the external plates under compression

The joint properties have been tabulated in Table 1. Also, the material properties of the members are tabulated in Table 2.

The numerical, experimental, and empirical f_{LJF} values of the 11 un-reinforced T, and Y-joints subjected to axial load are listed in Table 3. Mean Absolute Error (MAE) and Root Mean Square Error (RMSE) are 8.7 and 13.04, respectively. The comparison (Table 3) shows that the f_{LJF} values of the FE models are close to the corresponding f_{LJF} values of the experimental and empirical models. Consequently, the current developed numerical model precisely estimates the f_{LJF} of tubular joints in axial load. Figure 5 indicates the load-displacements curves of tubular X- and T-shaped joints reinforced with the external plates under axial load. The result shows that the initial joint stiffness of the FE models and experimental tests is very close, for all the reinforced tubular joints. Moreover, the present study of f_{LJF} in the joint is within the elastic range, the same as previous works (Nassiraei 2019). Consequently, the pres-

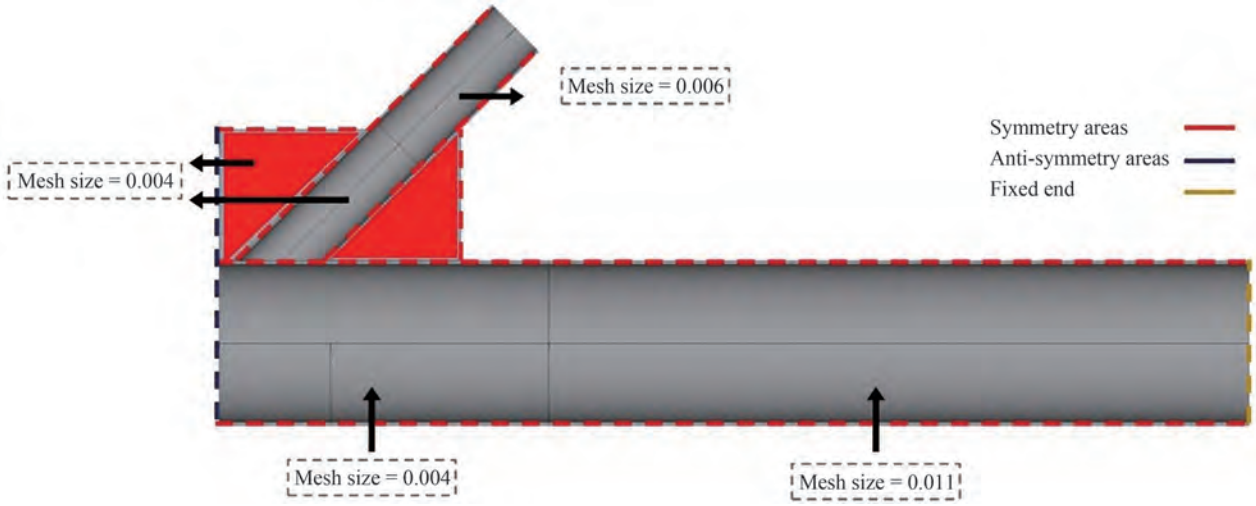

Figure 4 Mesh details and boundary conditions

Table 1 Geometrical parameters of the experimental tests

Specimen name	Researchers	D (mm)	Load Type	l_s (mm)	t_s (mm)	α	β	γ	τ	θ (°)
S1	Fessler et al. (1986)	132	Axial	–	–		0.33	10	0.39	90
S2				–	–		0.53	10	0.39	90
S3				–	–		0.76	10	0.48	90
S4				–	–		0.53	20	0.78	90
S5				–	–		0.76	20	0.96	90
S6				–	–		0.33	10	0.39	35
S7				–	–		0.33	10	0.39	50
S8				–	–		0.76	10	0.48	50
S9				–	–		0.53	15	0.59	50
S10				–	–		0.53	20	0.78	50
S11				–	–		0.76	20	0.96	50
S12	Li et al. (2018)	299.60	Compression	303.50	7.80	12.06	0.51	18.68	1.01	90
S13		300.40		437.3	7.90	11.96	0.73	18.70	1.00	90
S14	Ding et al. (2018)	304.00	Tension	152	8	11.86	0.25	18.68	0.71	90
S15		298.03		302	8	12.06	0.51	17.90	1.04	90
S16	Zhu et al. (2017)	298.2	Compression	71.5	5.3	12.07	0.25	26.62	1.10	90

Table 2 Material parameters of the members of the tests

Specimen	E_s (GPa)	E_1 (GPa)	E_0 (GPa)	f_{ys} (MPa)	f_{y1} (MPa)	f_{y0} (MPa)
S1 - S5	207	207	–	–	–	–
S6			–	–	–	–
S7 - S11			–	–	–	–
S12	194	192	212	325	316	301
S13	194	200	212	325	321	301
S14	200.3	222.3	246.5	267.7	313.3	358.3
S15	200.3	240	246.5	267.7	295	358.3
S16	227	224	229	345	470	322

Notes: The E_0, E_1 and E_s are the Yang's modulus of the chord, brace, and plate members, respectively. The f_{y0}, f_{y1} and f_{ys} are the yield stress of the chord, brace, and plate members, respectively.

ent numerical model of the reinforced tubular joints is accurate enough to generate safe f_{LJF} results.

5 Effect of geometrical parameters on the f_{LJF} and ψ

5.1 Details

One hundred fifty numerical models were generated, in ANSYS version 20, to investigate the effect of the brace angle (θ), joint geometry (τ, ζ, β, and γ) and the reinforcing plate (η and λ) on the f_{LJF} of the reinforced K-joints under axial load. The definition of the parameters is presented in

Table 3 Comparison of the results of the present FE model with the experimental data and the equation

Specimen	FE	Fessler Experimental	FE/Exp.	Fessler Equation	FE/Equation
S1	165	152	1.08	153	1.07
S2	113.76	105	1.08	103	1.10
S3	66.03	57	1.15	43	1.53
S4	396.03	430	0.92	456	0.86
S5	226.4	219	1.03	191	1.18
S6	50.43	52	0.97	48	1.05
S7	94.61	85	1.11	91	1.04
S8	37.69	34	1.11	24	1.57
S9	118.11	120	0.98	137	0.86
S10	222.97	239	0.93	254	0.88
S11	130.18	118	1.10	106	1.23

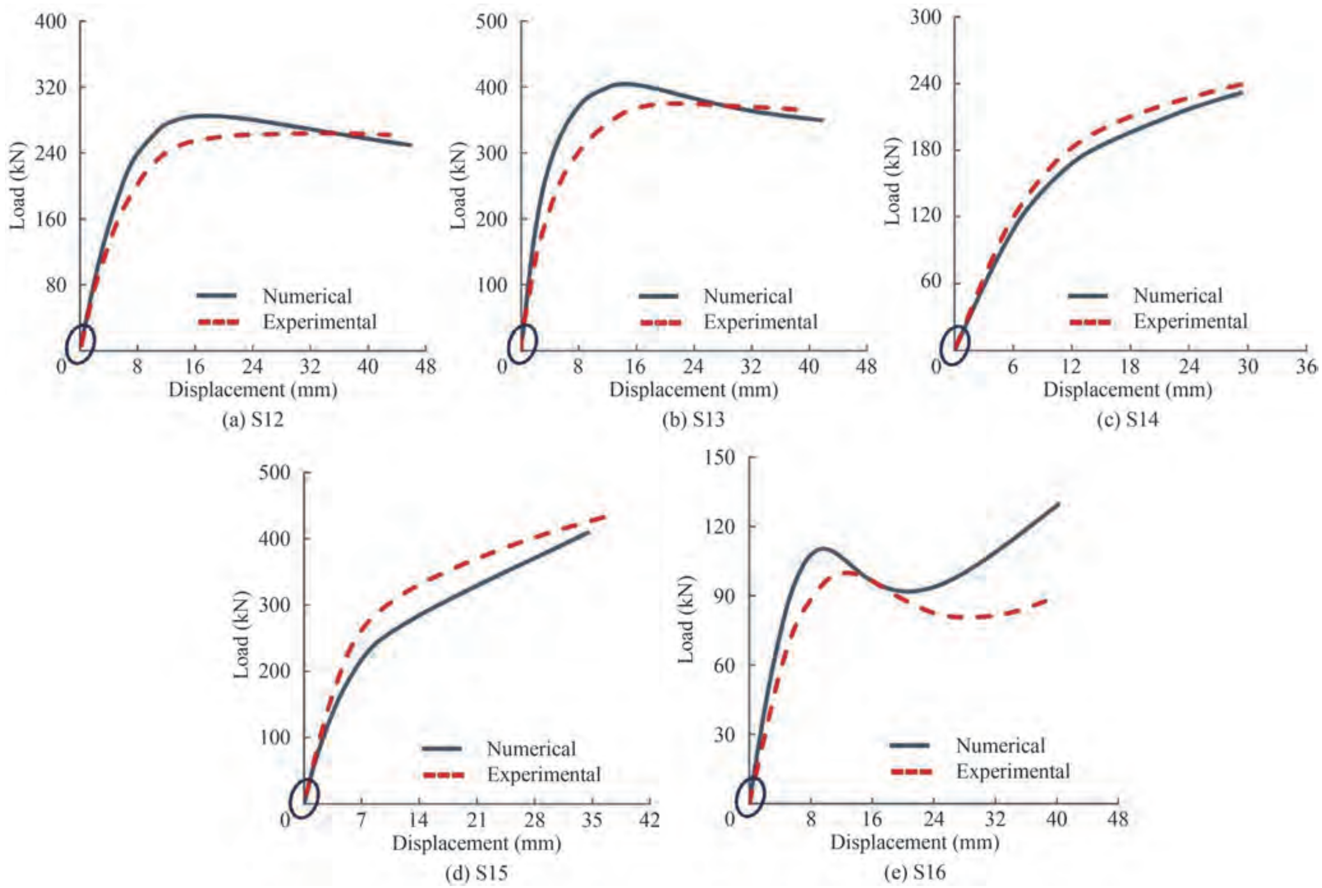

Figure 5 The comparison the present numerical results with the experimental data

Figure 1. The numerical models include three diverse η ratios, three different λ ratios, seven different τ proportions, five different θ ratios, five different ζ ratios, seven different γ ratios, and seven different β ratios. The elastic module of Young for the members and weld equals 207 GPa. To investigate the f_{LJF} of the reinforced K-joints with the corresponding un-reinforced joints, a new parameter χ is presented. The χ is defined to $f_{LJF,s}/f_{LJF,u}$. The $f_{LJF,s}$ is the f_{LJF} of the K- joint reinforced with the reinforcing plate. The $f_{LJF,u}$ is the f_{LJF} of the un-reinforced K-joint.

5.2 The effect of θ, η, and λ

Figure 6 shows that the increase of the θ leads to the increase of the f_{LJF}. Because, the increase of the θ leads to the decrease of the initial joint stiffens. Also, the external

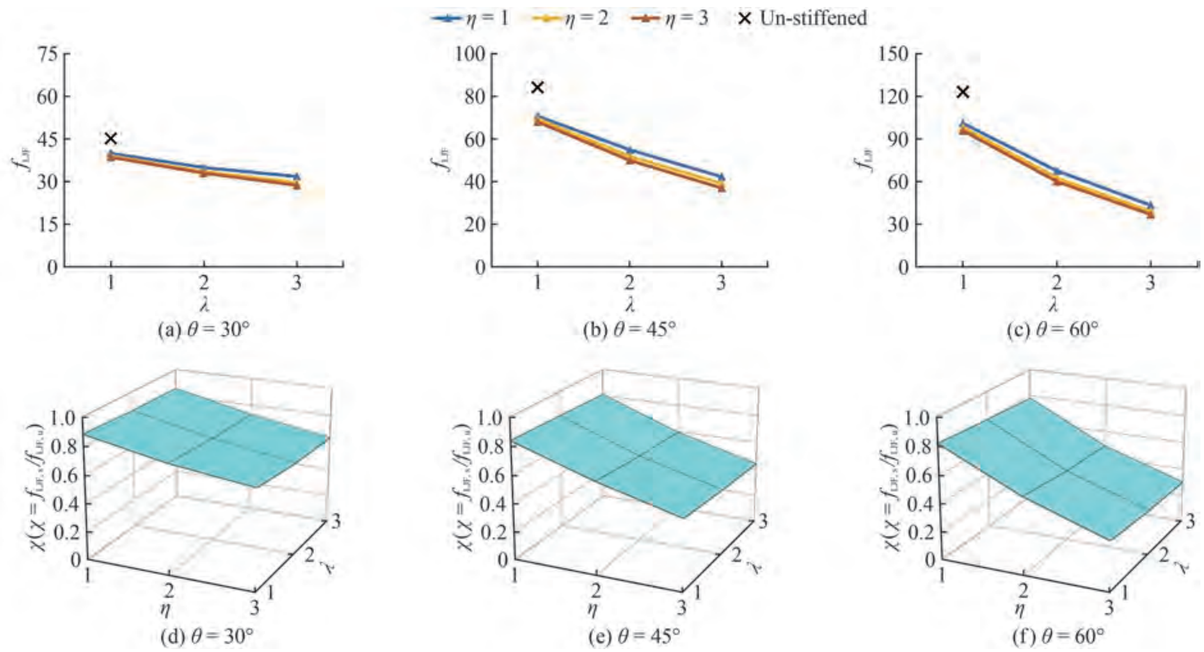

Figure 6 The effect of the θ, λ, and η on the f_{LJF} and the χ (f_{LJF} ratio of the reinforced to the corresponding un-reinforced joint) for the joints with $\tau = 0.8$, $\xi = 0.4$, $\gamma = 18$, and $\beta = 0.7$

plates have considerable effect on decreasing the f_{LJF}. Because in the reinforced joints, the reinforcing plates enhance the joints stiffness. The increase of the joint's stiffness leads to the decrease of the reshaping. Furthermore, the results indicate that the effect of the reinforcing plate thickness on the decrease of the f_{LJF} is more significant than the effect of the reinforcing plate length on the decrease of the f_{LJF}. Because, the main displacement happens in the joint intersection. Hence, using the reinforcing plate with more length cannot be very useful. Also, in the K-joint with bigger θ, the reducing effect of the stiffener plate on the f_{LJF} becomes more considerable. For example, in the reinforced joints with $\eta = 3$, $\lambda = 3$, $\gamma = 18$, $\beta = 0.7$, $\xi = 0.4$, and $\tau = 0.8$, when the θ is 30°, 45°, and 60° the χ (f_{LJF} ratio of the reinforced to the corresponding un-reinforced joints) is equal to 0.59, 0.44, and 0.30.

5.3 The effect of β, η, and λ

This section studies the effect of the β, η, *and* λ on the f_{LJF} and the χ in the joints with $\gamma = 32$, $\xi = 0.3$, $\tau = 0.5$, and $\theta = 40°$. Figure 7 illustrates that the increase of the β leads to the decrease of the f_{LJF}. Since, the brace diameter and the reinforcing plate length in the reinforced joints with higher β are bigger than the brace diameter and the reinforcing plate length in the corresponding reinforced joints with smaller β, respectively. The growth in these two parameters leads to the increase in the initial joint stiffness. In addition, the f_{LJF} of the reinforced K-joints is notably smaller than the f_{LJF} of the corresponding un-reinforced K-joints. Also, by decreasing the β value, the effect of the λ and η value on the f_{LJF} and χ become more significant. For example, in the joints with $\eta = 1$, $\lambda = 2$, $\gamma = 32$, $\xi = 0.3$, $\tau = 0.5$, and $\theta = 40°$ (Figures 7d-7f) the χ for the joints with $\beta = 0.2$, 0.5, and 0.8 is equal to 0.72, 0.87, and 0.91 respectively. As a result, the enhancing effect of the reinforcing plate is more significant for the joints with smaller β.

5.4 The effect of γ, η, and λ

This section investigates the effect of the γ, λ, *and* η on the f_{LJF} and the χ. Figure 8 presents the results for the joints with $\xi = 0.5$, $\beta = 0.3$, $\tau = 0.6$, and $\theta = 50°$ and different values of the γ, η, *and* λ. As it can be seen, the f_{LJF} of the un-reinforced joints is remarkably bigger than the f_{LJF} of the corresponding plate-reinforced joints. Also, by increasing the reinforcing plate size, the difference between the f_{LJF} of the un-reinforced and reinforced joints becomes bigger. Since, the bigger stiffener plates absorb more energy. Consequently, using the bigger plates leads to less reshaping and f_{LJF}. However, the effect of the reinforcing plate thickness on decreasing the f_{LJF} is more remarkable than the effect of the reinforcing plate length on decreasing the f_{LJF}.

The results indicate that the increase of the γ leads to the considerable decrease of the f_{LJF}. Because, the increase of the γ leads to the decrease of the thicknesses in both the chord and external plates. This results in the decrease of the joint stiffness. But, the effect of the γ on the χ can be ignored. For example, in the joints with $\eta = 2$, $\lambda = 3$, $\xi = 0.5$, $\beta = 0.3$, $\tau = 0.6$, and $\theta = 50°$, the χ is equal to 0.49 and 0.51 for the joints with γ equal to 15 and 20, respectively.

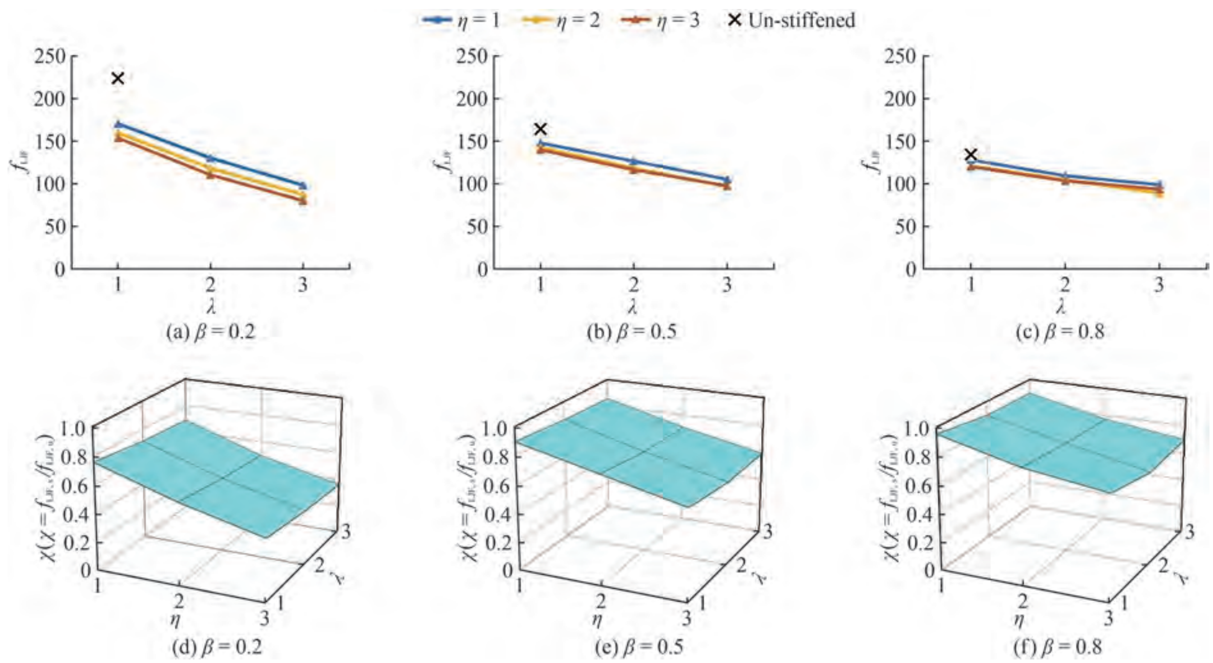

Figure 7 The effect of the β, λ, and η on the f_{LJF} and the χ (f_{LJF} proportion of the reinforced to the corresponding un-reinforced joint) for the joint with $\xi = 0.3$, $\tau = 0.5$, $\gamma = 32$, and $\theta = 40°$

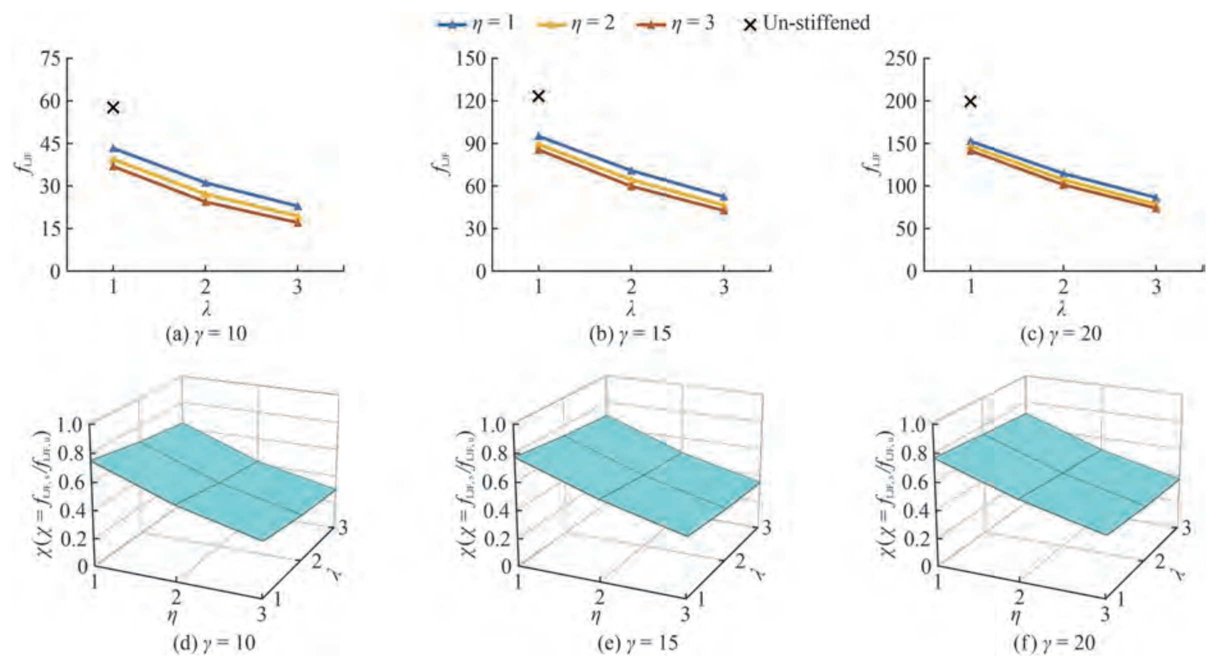

Figure 8 The effect of the γ, λ, and η on the f_{LJF} and the χ (f_{LJF} proportion of the reinforced to the corresponding un-reinforced joint) for the joint with $\xi = 0.5$, $\beta = 0.3$, $\tau = 0.6$, and $\theta = 50°$

5.5 The effect of τ, η, and λ

This section investigates the effect of τ, λ, and η on the f_{LJF} and χ in the joint with $\xi = 0.2$, $\beta = 0.4$, $\theta = 45°$, and $\gamma = 25$. Figure 9 indicates that LJF of the reinforced joints is notably smaller than the corresponding un-reinforced joints. For instance, the f_{LJF} of the reinforced joints with $\eta = 2$, $\lambda = 2$, $\tau = 0.7$, $\beta = 0.4$, $\gamma = 25$, $\theta = 45°$, and $\xi = 0.2$, (Figure 9e) is 59% of the f_{LJF} of the corresponding un-reinforced joints. Furthermore, the increase of the τ leads to the decrease of the f_{LJF}. Since, the increase of the τ leads to the increase of the brace thickness. The growth of this thickness results in the enhancement of joint stiffness. As it can be concluded, the change of the τ from 0.4 to 0.7 can result in more decrease in f_{LJF} rather than the change of the τ from 0.7 to 1.0.

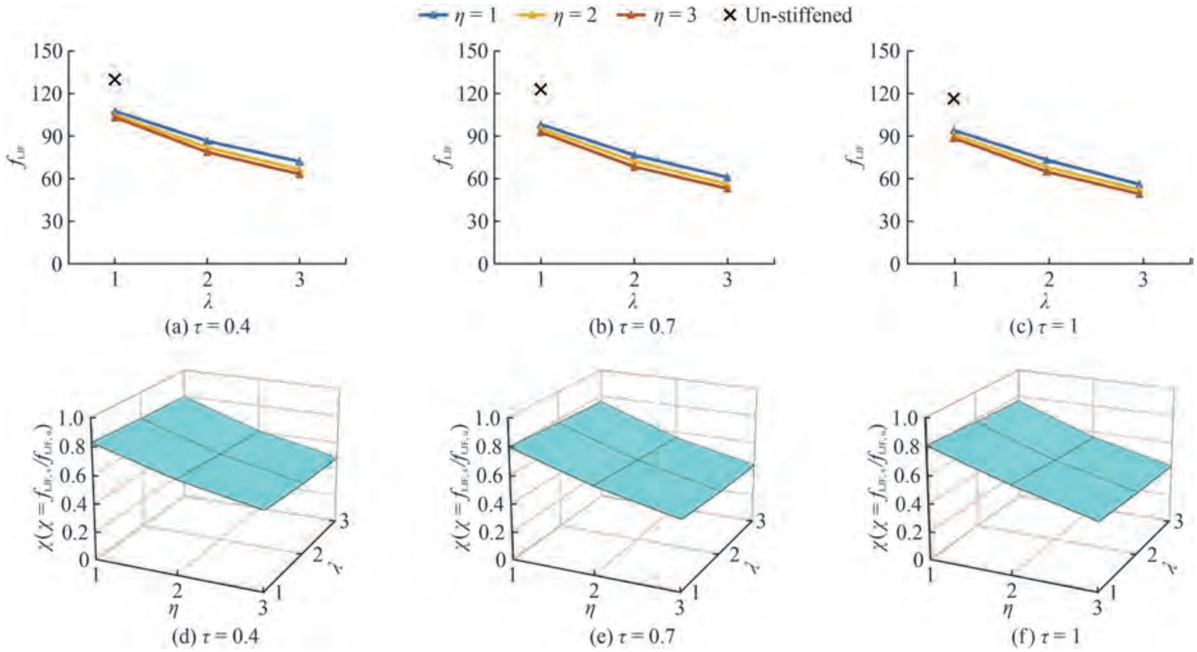

Figure 9 The effect of the τ, λ, and η on the f_{LJF} and the χ (f_{LJF} proportion of the reinforced to the corresponding un-reinforced joint) for the joint with $\xi = 0.2$, $\gamma = 25$, $\beta = 0.4$, and $\theta = 45°$

5.6 The effect of ξ, λ, and η

Figure 10 shows the ψ values for the joints with different values of the ξ, η, and λ. It can be observed that the increase of the ξ leads to a slight decrease of the ψ. For example, in the joints with $\eta = 1$, $\lambda = 3$, $\gamma = 12$, $\beta = 0.9$, $\tau = 0.9$, and $\theta = 60$, when the ξ is equal to 0.2, 0.4, and 0.6, the ψ is equal to 0.69, 0.67, and 0.65, respectively. Despite the ξ, the increase of the reinforcing plate size (η and λ) leads to the significant decrease of the ψ.

6 Design formula

No formula is available to determine the f_{LJF} in reinforced K-joints under axial load. Therefore, by using the obtained data of the current 150 FE models and SPSS (software package), parametric Eq. (5) is proposed for this aim.

In order to develop this parametric equation, multiple nonlinear regression analyses were performed by the statistical software package, SPSS. Values of dependent variable (i.e. f_{LJF} ratio) and independent variables (λ, η, θ, γ, β, and τ) constitute the input data imported in the form of a matrix. Every row of this matrix involves the information about the f_{LJF} ratio values in a reinforced K-joint having specific geometrical properties. The input matrix for derivation of the equation had 150 rows equation (the number of FE models) and 7 columns (equation the number of dependent and independent variables). Hence, the whole FE strength ratio database was arranged as 1 400 input matrices. When the dependent and independent variables are defined, a model expression must be built with defined parameters. Parameters of the model expression are unknown coefficients and exponents. The researcher must specify a starting value for each parameter, preferably as close as possible to the expected final solution. Poor starting values can result in failure to converge or in convergence on a solution that is local (rather than global) or is physically impossible. Various model expressions must be built to derive a

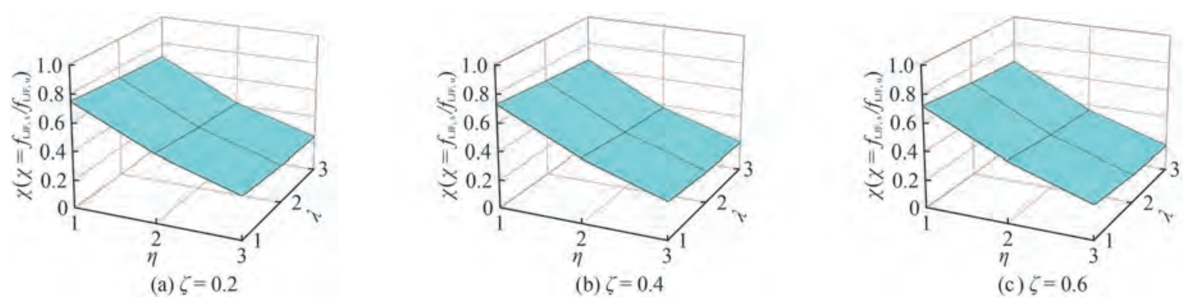

Figure 10 The effect of the ξ, λ, and η on the f_{LJF} and the χ (f_{LJF} proportion of the reinforced to the corresponding un-reinforced joint) for the joint with $\gamma = 12$, $\beta = 0.9$, $\tau = 0.9$, and $\theta = 60°$

parametric equation having a high coefficient of determination.

$$\chi = 1 - 1.04\gamma^{0.298}\beta^{-0.379}\tau^{0.2}\zeta^{0.071}\eta^{0.675}\lambda^{-0.223}\sin^{2.492}(0.222\beta^{10} + 0.064\lambda^{0.939} + 0.116\sin^{-0.847}) - 65.67\sin^{-0.005} + 65.48\gamma^{0.002};\ R^2 = 0.91 \quad (4)$$

where χ is the f_{LJF} ratio of the retrofitted K-joints to the corresponding un-retrofitted joint under axial load. The R^2 is the determination factor. Its value is close to 1. The application range for the use of Eq. (4) is as follow:

$$\begin{aligned} 1 \leqslant \eta \leqslant 3, \\ 1 \leqslant \lambda \leqslant 3 \\ 0.4 \leqslant \tau \leqslant 1.0, \\ 10 \leqslant \gamma \leqslant 32, \\ 0.2 \leqslant \beta \leqslant 0.9, \\ 30^\circ \leqslant \theta \leqslant 75^\circ, \\ 0.2 \leqslant \zeta \leqslant 0.6. \end{aligned} \quad (5)$$

If consider P and M as the predicted values and the measured value, respectively, the UK Department of Energy suggests the below standard.

- If [P/M < 0.8] ⩽ 5%; and [P/M < 1.0] ⩽ 25%, the formula is accepted. If also, [P/M > 1.5] ⩾ 50%, the equation is taken as commonly circumspect.
- If 5% < [P/M < 0.8] ⩽ 7.5%, and/or 25% < [P/M < 1.0] ⩽ 30%, the formula is taken as borderline. consequently, more evaluation should be conducted.
- Otherwise, the established equation cannot be approved. Because, it is too optimistic.

It should be noted that according the recommendation of Bomel Consulting Engineers (1994), P/R < 1.0 can be eliminated in the assessment. Evaluating Eq. (4) according to the UK DoE (1983) standard is listed in Table 4. It can be seen that the equation needs revision. To revise Eq. (4), the $f_{LJF,s}$ values calculated from the equation was multiplied by a factor in such a way that resulted $f_{LJF,s}$ values satisfying the UK DoE (1983)acceptance standard. The design factor can be determined as follows:

$$\text{Design factor} = f_{LJF,s\,(Design)} / f_{LJF,s\,(Eq.(4))} \quad (6)$$

where the values of $f_{LJF,s\ (Eq.(4)}$ are calcula ted from the derived equation and the values of $f_{LJF,s\ (Design)}$ are expected to satisfy the UK DoE (1983) standard. The following formula is suggested for the design aims.

$$f_{LJF,s\,(Design)} = 1.02\, f_{LJF,s\,(Eq.(4))} \quad (7)$$

Table 4 Assessment of developed equations based on the UK Department of Energy (1983) criteria

Equation	UK DoE Conditions				Decision		Design factor
	%P/R < 0.8		%P/R > 1.5				
	Before the revision	After the revision	Before the revision	After the revision	Before the revision	After the revision	
Eq. (5)	6.6% > 5% Not OK	4.4% < 5% OK	0.0% < 50% OK	0.0% < 50% OK	Needs revision	Accept	1.02

The results of the evaluation for the revised equation based on the UK DoE (1983) standard are tabulated in Table 4.

Mean Absolute Error (MAE) and Root Mean Square Error (RMSE) are 0.03 and 0.04, respectively. In Figure 11, the f_{LJF} ratios extracted by the proposed equation are compared with the corresponding values obtained from FE analyses. The value of R^2 (R^2 = 0.91), evaluating the equations based on the UK DoE standard, and Figure 11 indicate that the proposed formula is accurate to produce reliable data.

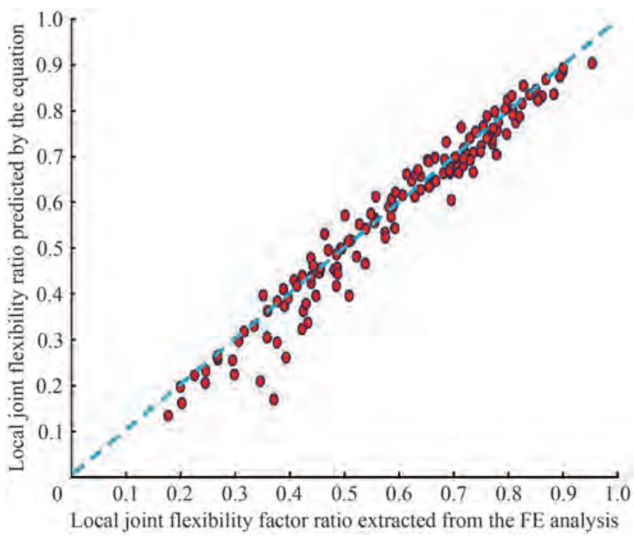

Figure 11 Comparison of the χ (f_{LJF} ratio) predicted by the proposed formula with the associated values extracted from the FE models for the stiffened K-joint

7 Conclusions

A total of 150 numerical models, after validation with several experimental tests, was generated to investigate the effect of the joint geometry, the brace angle, and the stiffener plate size on the f_{LJF} of the tubular K-joints under axial load. The main conclusions are as follows:

• Verification of the present numerical models with experimental results indicates that the FE model can well predict the f_{LJF} of un-reinforced and plate reinforced K-joints in axial loads. In addition, the reinforcing plate thickness and the reinforcing plate length have significant effect in the decrease of the f_{LJF}.

• The results indicated that using the external plates can decrease 81% of the f_{LJF}.

• The increase of the θ results in the increase of the f_{LJF}. Moreover, in the joints with bigger θ, the reducing effect of the stiffener plate on the f_{LJF} becomes more significant.

• The increase of the β leads to the decrease of the f_{LJF}. Because, the brace diameter and the reinforcing plate length in the reinforced joints with higher β are bigger than the brace diameter and the reinforcing plate length in the corresponding joints with smaller β, respectively. The growth in these two parameters leads to the increase in the joint stiffness. Also, by decreasing the β value, the effect of the λ and η value on the f_{LJF} and f_{LJF} ratio (χ) becomes more considerable. Consequently, the reinforcing effect of the reinforcing plate is more remarkable for the joints with smaller β.

• The increase of the γ leads to the considerable decrease in the f_{LJF}. Because, the increase of the γ leads to the decrease of the thicknesses in both the chord and external plates. However, the effect of the γ on the χ can be ignored. The increase of the ξ leads to a slight decrease of the χ. The increase of the τ leads to the decrease of the f_{LJF} in the reinforced joints.

• A design formula is proposed for determining the f_{LJF} in K-joints reinforced with the external plates under axial load. High determination factor (R^2 = 0.91), accepting the UK DoE criteria, and good match compared to corresponding values in a figure indicted that the proposed formula can be reliably utilized for designing and reinforcing tubular K-joints.

References

Ahmadi H, Mayeli V (2018) Probabilistic analysis of the local joint flexibility in two-planar tubular DK-joints of offshore jacket structures under in-plane bending loads. Applied ocean research 81: 126-140. https://doi.org/10.1016/j.apor.2018.10.011

American Welding Society (AWS). Structural welding code: AWS D 1.1. 2005

Asgarian B, Mokarram V, Alanjari P (2014) Local joint flexibility equations for YT and K-type tubular joints. Ocean Syst. Eng. 4(2): 151-167

Bomel Consulting Engineers. Assessment of SCF Equations Using Shell/KSEPL Finite Element Data. C5970R02.01 REV C 1994

Bouwkamp JG, Hollings JP, Masion BF, Row DG (1980) Effect of Joint Flexibility on the Response of Offshore Structures. Offshore Technology Conference (OTC), Houston, Texas 455-464

Buitrago J, BE Healy, TY Chang (1993) Local joint flexibility of tubular joints

Chaubey AK, Kumar A, Chakrabarti A (2018a) Vibration of laminated composite shells with cutouts and concentrated mass. AIAA Journal 56(4): 1662-1678

Chaubey AK, Kumar A, Mishra SS (2018b) Dynamic analysis of laminated composite rhombic elliptic paraboloid due to mass variation. Journal of Aerospace Engineering 31(5): 04018059

Chen B, Hu Y, Tan M (1990) Local joint flexibility of tubular joints of offshore structures. Marine Structures 3: 177-97

Ding Y, Zhu L, Zhang K, Bai Y, Sun H (2018) CHS X-joints strengthened by external stiffeners under brace axial tension. Engineering structures 171: 445-452

Efthymiou M (1985) Local Rotational Stiffness of Un-stiffens Tubular Joints, RKER report 185-199

Fessler H, Mockford PB, Webster JJ (1986a) Parametric equations for the flexibility matrices of multi-brace tubular joints in offshore structures. Proc Inst Civ Eng 81(4): 675-696

Fessler H, Mockford PB, Webster JJ (1986b) Parametric equations for the flexibility matrices of single brace tubular joints in offshore structures. Proc. Inst. Civ. Eng. 81: 659-673

Gao F, Hu B, Zhu HP (2013) Parametric equations to predict LJF of completely overlapped tubular joints under lap brace axial loading. Journal of constructional steel research 89: 284-292. https://doi.org/10.1016/j.jcsr.2013.07.010

Íñiguez-Macedo S, Lostado-Lorza R, Escribano-García R, Martínez-Calvo MÁ (2019) Finite element model updating combined with multi-response optimization for hyper-elastic materials characterization. Materials 12(7) 1019

Khan I, Smith K, Gunn M (2016) The role of local joint flexibility (LJF) in the structural assessments of ageing offshore structures. In The Twelfth ISOPE Pacific/Asia Offshore Mechanics Symposium. OnePetro

Khan R, Smithm K, Kraincanicm I (2018) Improved LJF equations for the uni-planar gapped K-type tubular joints of ageing fixed steel offshore platforms. J. Mar. Eng. Tech. 17(3): 121-136

Kumar A, Chakrabarti A, Bhargava P (2015) Vibration analysis of laminated composite skew cylindrical shells using higher order shear deformation theory. Journal of Vibration and Control 21(4): 725-735

Li W, Zhang S, Huo W, Bai Y, Zhu L (2018) Axial compression capacity of steel CHS X-joints strengthened with external stiffeners. Journal of constructional steel research 141: 156-166

Lostado Lorza R, Corral Bobadilla M, Martínez Calvo MÁ, Villanueva Roldán PM (2017) Residual stresses with time-independent cyclic plasticity in finite element analysis of welded joints. Metals 7(4):136

Lostado Lorza R, Escribano García R, Fernandez Martinez R, Martínez Calvo MÁ (2018) Using genetic algorithms with multi-objective optimization to adjust finite element models of welded joints. Metals 8(4): 230

Lostado R, Martinez RF, Mac Donald BJ, Villanueva PM (2015) Combining soft computing techniques and the finite element method to design and optimize complex welded products. Integrated Computer-Aided Engineering 22(2): 153-170

Lu Y, Liu K, Wang Z, Tang W (2020) Dynamic behavior of scaled tubular K-joints subjected to impact loads. Marine Structures 69: 102685

Martins JL, Silva RP, (2015) October. Evaluation of Local Joint Flexibility Effects in Fixed Oil Platforms. In OTC Brasil. OnePetro

Mishra BB, Kumar A, Zaburko J, Sadowska-Buraczewska B, Barnat-Hunek D (2021) Dynamic response of angle ply laminates with uncertainties using MARS, ANN-PSO, GPR and ANFIS. Materials 14(2) 395

Nassiraei H (2017) Development of Experimental and Numerical Models for the Study of Ultimate Strength of Tubular Joint Reinforced with External Plates, thesis

Nassiraei H (2019a) Local joint flexibility of CHS X-joints reinforced with collar plates in jacket structures subjected to axial load. Applied ocean research 93: 101961. https://doi.org/10.1016/j.apor.2019.101961

Nassiraei H (2019b) Static strength of tubular T/Y-joints reinforced with collar plates at fire induced elevated temperature. Marine Structures 67:102635. https://doi.org/10.1016/j.marstruc.2019.102635

Nassiraei H (2020) Local joint flexibility of CHS T/Y-connections strengthened with collar plate under in-plane bending load: parametric study of geometrical effects and design formulation. Ocean Engineering 202: 107054. https://doi.org/10.1016/j.oceaneng.2020.107054

Nassiraei H (2022) Geometrical effects on the LJF of tubular T/Y-joints with doubler plate in offshore wind turbines. Ships and Offshore Structures 17(3): 481-491. https://doi.org/10.1080/17445302.2020.1835051

Nassiraei H, Lotfollahi-Yaghin MA, Ahmadi H (2016) Static strength of doubler plate reinforced tubular T/Y-joints subjected to brace compressive loading: Study of geometrical effects and parametric formulation. Thin-Walled Structures 107: 231-247. https://doi.org/10.1016/j.tws.2016.06.009

Nassiraei H, Lotfollahi-Yaghin MA, Ahmadi H, Zhu L (2017) Static strength of doubler plate reinforced tubular T/Y-joints under in-plane bending load. Journal of Constructional Steel Research 136: 49-64. https://doi.org/10.1016/j.jcsr.2017.05.009

Nassiraei H, Lotfollahi-Yaghin MA, Neshaei SA, Zhu L (2018) Structural behavior of tubular X-joints strengthened with collar plate under axially compressive load at elevated temperatures. Marine Structures 61: 46-61. https://doi.org/10.1016/j.marstruc.2018.03.012

Nassiraei H, Mojtahedi A, Lotfollahi-Yaghin MA, Zhu L (2019) Capacity of tubular X-joints reinforced with collar plates under tensile brace loading at elevated temperatures. Thin-Walled Structures 142: 426-443. https://doi.org/10.1016/j.tws.2019.04.042

Nassiraei H, Rezadoost P (2020) Stress concentration factors in tubular T/Y-joints strengthened with FRP subjected to compressive load in offshore structures. International Journal of Fatigue 140: 105719. https://doi.org/10.1016/j.ijfatigue.2020.105719

Nassiraei H, Rezadoost P (2021a) Local joint flexibility of tubular X-joints stiffened with external ring or external plates. Marine Structures 80: 103085. https://doi.org/10.1016/j.marstruc.2021.103085

Nassiraei H, Rezadoost P (2021b) Local joint flexibility of tubular T/Y-joints retrofitted with GFRP under in-plane bending moment. Marine Structures 77: 102936. https://doi.org/10.1016/j.marstruc.2021.102936

Nassiraei H, Rezadoost P (2021c) Static capacity of tubular X-joints reinforced with fiber reinforced polymer subjected to compressive load. Engineering Structures 236: 112041. https://doi.org/10.1016/j.engstruct.2021.112041

Nassiraei H, Rezadoost P (2021d) SCFs in tubular X-connections retrofitted with FRP under in-plane bending load. Composite Structures 274: 114314. https://doi.org/10.1016/j.compstruct.2021.114314

Nassiraei H, Rezadoost P (2021e) SCFs in tubular X-joints retrofitted with FRP under out-of-plane bending moment. Marine Structures 79: 103010. https://doi.org/10.1016/j.marstruc.2021.103010

Nassiraei H, Rezadoost P (2021f) Stress concentration factors in tubular X-connections retrofitted with FRP under compressive load. Ocean Engineering 229: 108562. https://doi.org/10.1016/j.oceaneng.2020.108562

Nassiraei H, Rezadoost P (2021g) Stress concentration factors in tubular T/Y-connections reinforced with FRP under in-plane bending load. Marine Structures 76: 102871. https://doi.org/10.1016/j.marstruc.2020.102871

Nassiraei H, Rezadoost P (2021h) Parametric study and formula for SCFs of FRP-strengthened CHS T/Y-joints under out-of-plane bending load. Ocean Engineering 221: 108313. https://doi.org/10.1016/j.oceaneng.2020.108313

Nassiraei H, Rezadoost P (2022a) Static capacity of tubular X-joints stiffened with external ring subjected to compressive loading: study of geometrical effects and parametric formulation. Sharif Journal of Civil Engineering. https://doi.org/10.24200/J30.2022.59133.3029

Nassiraei H, Rezadoost P (2022b) Probabilistic analysis of the ultimate strength of tubular X-joints stiffened with outer ring at ambient and elevated temperatures. Ocean Engineering 248: 110744. https://doi.org/10.1016/j.oceaneng.2022.110744

Nassiraei H, Yara A (2022) Local joint flexibility of tubular K-joints reinforced with external plates under IPB loads. Marine Structures 84: 103199. https://doi.org/10.1016/j.marstruc.2022.103199

UK Department of Energy. Background notes to the fatigue guidance of offshore tubular connections. London, UK 1983

Underwater Engineering Group, Design of Tubular Joint for Offshore Structures. UEG/CIRIA, London, UK 1985

Zhu L, Song Q, Bai Y, Wei Y, Ma L (2017) Capacity of steel CHS T-Joints strengthened with external stiffeners under axial compression. Thin-Walled Struct. 113 (2017) 39-46. https://doi.org/10.1016/j.tws.2017.01.007